ABSTRACT

MATHEMATICAL ANALYSIS OF TSUNAMI AND ROGUE WAVES

by

Bradley Eidschun

April, 2012

Chair: Dr. David W. Pravica

Major Department: Mathematics

In this thesis both forced and non-linear wave equations will be studied. Actual data from tsunami and rogue waves will be used and a signal analysis will be performed using wavelets. Main results show that a different choice of wavelet leads to different efficiencies occurring in the signal recovery process.

MATHEMATICAL ANALYSIS OF TSUNAMI AND ROGUE WAVES

A Thesis

Presented to

The Faculty of the Department of Mathematics

East Carolina University

In Partial Fulfillment

of the Requirements for the Degree

Master of Arts in Mathematics

by

Bradley Eidschun

April, 2012

MATHEMATICAL ANALYSIS OF TSUNAMI AND ROGUE WAVES

by

Bradley Eidschun

APPROVED BY:

DIRECTOR OF THESIS:

Dr. David W. Pravica

COMMITTEE MEMBER:

Dr. Chris Jantzen

COMMITTEE MEMBER:

Dr. Michael Spurr

COMMITTEE MEMBER:

Dr. Gregory Lapicki

CHAIR OF THE DEPARTMENT
OF MATHEMATICS:

Dr. Johannes Hattingh

DEAN OF THE
GRADUATE SCHOOL:

Dr. Paul Gemperline

ACKNOWLEDGEMENTS

I would like to thank all of the people involved in the creation of this work. First and foremost, thank you to Dr. Pravica, for taking a chance on me and guiding me through the research and writing, in addition to making the whole experience pretty fun. He is also responsible for the programs that yielded charts for the numerical data. Also, hey, we got a poster! Yes! Thank you to my colleagues in the ECU Mathematics Department for seeing that my stress level was mitigated enough to keep me from also having to be committed to a psychiatric ward and given crazy pills. Thank you to my family for attempting to proofread this work (I know you guys don't understand any of it at all, but thanks for the effort!) and to my friends for enduring my requests to listen to my presentations.

Finally, I would to thank Dr. George Mongov (at NOAA) and Dr. Sverre Haver (at STATOIL, Norway) for providing data that was studied and displayed in this thesis. Let me also thank Dr. Michael J. Spurr and Dr. Njina Randriampiry for allowing the use of results of their recent research work.

TABLE OF CONTENTS

CHAPTER 1: Introduction

From reference [1], we define the d'Alembertian on $\mathbb{R}^{n+1}$:

$$\Box^2 \equiv \nabla^2 - \frac{1}{v^2}\frac{\partial^2}{\partial t^2} = \sum_{j=1}^{n} \frac{\partial^2}{\partial x_j^2} - \frac{1}{v^2}\frac{\partial^2}{\partial t^2} , \tag{1.1}$$

where ∇ is the gradient, and where v is the speed of the wave in the material being studied. The gradient of a function f in $\mathbb{R}^2$ is defined as

$$\nabla f(x,y) = \frac{\partial f}{\partial x} + \frac{\partial f}{\partial y} = f_x(x,y) + f_y(x,y) .$$

The gradient of a function is simply a vector having coordinate components that are partial derivatives of that function with respect to its variables. The gradient is described in physics as the rate at which a physical quantity, such as temperature or pressure, increases or decreases relative to changes in a given variable.

In this thesis we study the **wave equation**, which is an important partial differential equation that describes propagation of wave amplitudes ψ with speed v:

$$\nabla^2\psi = \frac{1}{v^2}\frac{\partial^2\psi}{\partial t^2} \qquad \text{or equivalently} \qquad \frac{\partial^2\psi}{\partial t^2} = v^2\nabla^2\psi .$$

A more compact form of the wave equation is given by:

$$\Box^2\psi = 0 , \tag{1.2}$$

where $\Box^2$ is the d'Alembertian defined in (1.1). Eqn.(1.2) represents the wave equation in n dimensional space. In a medium with constant speed v, it is invariant under space-time translations and rotations, and thus it is a naturally occuring equation.

CHAPTER 2: Derivation of the wave equation

The wave equation in n dimensions is known to model many types of vibrations found in physics [1]. In order to explain some of the concepts covered later, we will present various derivations of the wave equations. We will begin with the simplest case in order to build a good foundation for understanding wave propagation. This leads us to a discussion of the one-dimensional wave equation on a string. Here, our goal is to find some function $u(x,t)$ that satisfies the wave equation $u_{tt} = v^2 u_{xx}$ [2] where we use the notation

$$u_{xx} \equiv \frac{\partial^2 u}{\partial x^2} \qquad \text{and} \qquad u_{tt} = \frac{\partial^2 u}{\partial t^2} .$$

2.1 1D Wave Equation

Consider a tightly stretched string along the x-axis with an inconsequential thickness. Any force exerted on the string will cause displacement in the (x,y) plane. Say $u(x,t)$ is our displacement in the y direction from its equilibrium position. We think of u as the amplitude of the wave. Now we will let T be the equilibrium tension on the string, and consider neighboring points x and $x+dx$ (see Figure 1); note that the forces at these two points is usually different. Now, we want to assume there is no net sideways acceleration. Hence, the sum of our horizontal forces will be 0 at any time t, leading to the equality:

$$T(x,t) \cdot \cos(\theta(x,t)) = T(x+dx,t) \cdot \cos(\theta(x+dx,t)) . \tag{2.1}$$

Thus the force in the upward direction is $T(x+dx) \cdot \sin(\theta(x+dx))$, while the downward component of force is given by $T(x) \cdot \sin(\theta(x))$ (suppressing the t dependence).

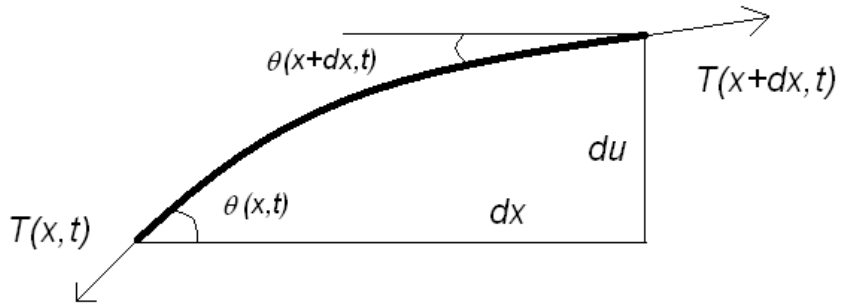

Figure 1: Tension T, angle θ, height du and width dx at a fixed moment of time t, on a linear interval $[x,\ x+dx]$.

Thus the sum of forces in the vertical direction is given by

$$dF \ = \ T(x+dx)\cdot\sin(\theta(x+dx)) \ - \ T(x)\cdot\sin(\theta(x)) \ . \tag{2.2}$$

Thus there is a net vertical force dF on the string element on the interval $[x, x+dx]$. Now if we make a small amplitude approximation ($|u| \ll 1$, $|\theta| \ll 1$):

$$T(x)\cdot(1-\theta^2(x)/2) \ \approx \ T(x+dx)\cdot(1-\theta^2(x+dx)/2) \ ,$$

using a Taylor expansion. Then our sum of forces is now approximately

$$dF \ \approx \ T(x+dx)\cdot\theta(x+dx) - T(x)\cdot\theta(x) \ .$$

This allows us to make yet another assumption about the sum of our forces:

$$dF \ \approx \ T(x+dx)\cdot\tan(\theta(x+dx)) \ - \ T(x)\cdot\tan(\theta(x)) \ . \tag{2.3}$$

Notice that from (2.2) to (2.3) we have replaced sines with tangents. The key to the possibility of this lies in the definition of the tangent function:

$$\tan(\theta) = \frac{\sin(\theta)}{\cos(\theta)}$$

In order for $\tan(\theta)$ to be approximately equal to $\sin(\theta)$, then $\cos(\theta)$ would have to be very close to 1. On the interval $[0, 2\pi)$, this only happens when θ is near zero. So for our approximation, the vibrations on the string would have to be very small. This actually makes sense. Think about a guitar string. When a guitar string is plucked, the vibrations that travel through it are nearly imperceptible.

We know that $\tan(\theta(x))$ is the slope of our string at x. From calculus, we know that the slope of a tangent line at a point is a derivative; thus (suppressing the t dependence):

$$u_x(x) \;=\; \frac{du}{dx} \;=\; \tan(\theta(x)) \;.$$

From this observation, our force now looks like:

$$dF \;\approx\; T(x+dx)\cdot u(x+dx) \;-\; T(x)\cdot u(x) \;.$$

If we multiply the right hand side by dx/dx, we get:

$$dF \;\approx\; d\left(T(x)\cdot u(x)\right)/dx \;=\; \left(T(x)\cdot u(x)\right)_x \;.$$

Now that we have an equation for the sum of our forces, we can utilize Newton's second law: $F = ma$, which means that the sum of forces on the string element is equal to its mass times its acceleration. This can also be reexpressed as $a = F/m$, which says that the acceleration of the string element is equal to the sum of forces on

it divided by its inertial mass.

We will use $\rho(x)$ for the mass density, also referred to as the mass per unit length. Then the mass of the string element on $[x, x+dx]$ is $dm \approx \rho(x) \cdot dx$. In addition, $f(x)$ is used for the body-force density, ie. $dF \approx f(x) \cdot dx$. Putting it all together yields:

$$(T(x)\, u_x)\, dx \;+\; f(x)\, dx \;=\; (\rho(x)\, dx) \cdot u_{tt}\ , \tag{2.4}$$

Now if we divide everything by the mass $\rho\, dx$, we end up with

$$\frac{T}{\rho}\, u_{xx} \;+\; \frac{f}{\rho} \;=\; u_{tt}\ . \tag{2.5}$$

Define the functions $v(x) \equiv \sqrt{T/\rho}$ and $g(x) \equiv f/\rho$. Substituting these into Eq.(2.5) yields the following expression for the acceleration of the string experienced at position x and time t:

$$u_{tt} \;=\; v^2\, u_{xx} \;+\; g\ . \tag{2.6}$$

Rearrangment gives

$$u_{tt} \;-\; v^2\, u_{xx} \;=\; g\ . \tag{2.7}$$

which represents a forced wave equation in one (space) dimension.

The methods used to derive the equation in Eq.(2.7) can be applied to a slightly more complex wave system; thus we proceed to our derivation of the wave equation in two dimensions.

2.2 2-D Wave Equation

Assume that we are working with a rectangular elastic sheet rather than a string this time. Just like we did with our string, we are going to apply Newton's Law ($F = ma$)

to a small square of elastic material; here we will assume the sides are parallel with the x and y axes. Recall that in our string derivation, we assigned a function to our vertical displacement; here we can do so again in this case. Say $u(x, y, t)$ is the displacement in the y direction. Also, say our left and right hand edges have length dy while the top and bottom sides have length dx. We will assume the displacement is small enough so as not to vary the tension, and that the sheet oscillates strictly up and down, while not being tugged to any one side. The total force on the left edge, at any fixed moment t in time, is $T(x, y, t)\, dy$, perpendicular to the edge dy; similar to before, we are using T for the tension per unit cross-section length, meaning that the longer a section taken, the more force is exherted by the material. Now, factoring in the slope of the sheet in the direction of the force, $Tdy\dfrac{\partial u(x, y, t)}{\partial x}$ is the vertically downward component of the force. By a similar argument, we can say that the total force acting on the right hand edge must also be $T(x + dx, y, t)\, dy$; now factoring in the slope of the sheet in the direction of the force, we arrive at $Tdy\dfrac{\partial u(x + dx, y, t)}{\partial x}$, which is the vertically upward component of our force.

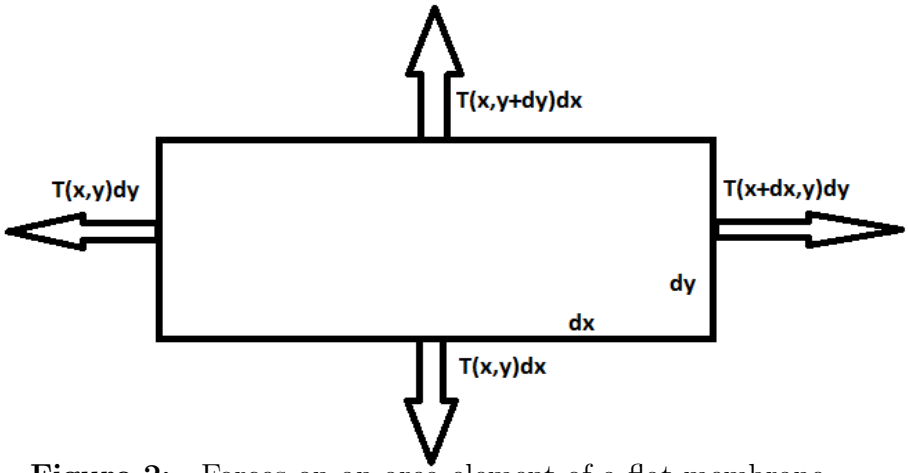

Figure 2: Forces on an area element of a flat membrane.

The net upward force acting on the left and right sides of our sheet now is the difference between our upward and downward vertical forces:

$$\begin{aligned} dF_x &= T dy \, \frac{\partial u(x+dx,y,t)}{\partial x} \; - \; T dy \, \frac{\partial u(x,y,t)}{\partial x} \\ &= T dy \, \left(\frac{\partial u(x+dx,y,t)}{\partial x} \; - \; \frac{\partial u(x,y,t)}{\partial x} \right) \\ &= T dy dx \, \left(\frac{\partial^2 u}{\partial x^2} \right) \; . \end{aligned}$$

But what about the other two sides of the elastic sheet element? Say we keep our tension force at T. Then our total force on, say, the upper edge would be $T(x,y)dx$, perpendicular to the edge dx. If we factor the slope of the sheet in the direction of the force, $Tdx\dfrac{\partial u(x,y,t)}{\partial y}$ is the vertically downward component of our force while $Tdx\dfrac{\partial u(x,y+dy,t)}{\partial y}$ is the vertically upward component of our force. Our net force now is as follows:

$$\begin{aligned} dF_y &= T dx \, \frac{\partial u(x,y+dy,t)}{\partial y} \; - \; T dx \, \frac{\partial u(x,y,t)}{\partial y} \\ &= T dx \, \left(\frac{\partial u(x,y+dy,t)}{\partial y} \; - \; \frac{\partial u(x,y,t)}{\partial y} \right) \\ &= T dy dx \, \left(\frac{\partial^2 u}{\partial y^2} \right) \; . \end{aligned}$$

Say the mass of our little square elastic sheet is $dm \approx \rho \, dxdy$, where ρ is the mass per unit area. Also note that our upward acceleration is $a = \partial^2 u / \partial t^2$. Now, using $F = ma$, in the form: $dF_x + dF_y = dm \cdot a$, we have,

$$\begin{aligned} T dy dx \left(\frac{\partial^2 u}{\partial x^2} \right) + T dy dx \left(\frac{\partial^2 u}{\partial y^2} \right) &= \rho \, dxdy \, \left(\frac{\partial^2 u}{\partial t^2} \right) \\ \Rightarrow \quad T \left(\frac{\partial^2 u}{\partial x^2} \right) \; + \; T \left(\frac{\partial^2 u}{\partial y^2} \right) &= \rho \left(\frac{\partial^2 u}{\partial t^2} \right) \\ \Rightarrow \quad \left(\frac{\partial^2 u}{\partial x^2} \right) \; + \; \left(\frac{\partial^2 u}{\partial y^2} \right) &= \frac{\rho}{T} \left(\frac{\partial^2 u}{\partial t^2} \right) \\ \Rightarrow \quad \left(\frac{\partial^2 u}{\partial x^2} \right) + \left(\frac{\partial^2 u}{\partial y^2} \right) &= \frac{1}{v^2} \left(\frac{\partial^2 u}{\partial t^2} \right) \; . \end{aligned}$$

Here $v^2 = T/\rho$. Thus we have the wave equation in the second dimension!

2.3 3D Wave Equation restricted to a sphere

We are now going to derive the wave equation in three dimensions where propagation occurs only on a sphere of radius r. Our approach will use spherical coordinates instead of Cartesian. Let us consider elastic waves on the surface of a sphere. Here we use θ to measure latitude (with 0 as the north pole and π as the south pole) and ϕ to measure our longitude. Take a small elastic area element from on the sphere. It will be bounded by longitude lines ϕ and $\phi + d\phi$ as well as latitude lines θ and $\theta + d\theta$. We are setting $dr = 0$ in these cases.

For a sphere of radius r, the lengths of the sides of an elastic volume element are: $rd\theta$ and $r \sin\theta \, d\phi$. Let T be the tension per unit cross-sectional area. With our longitude side, length $rd\theta$, we need to figure out the deviation from the horizontal. Let us suppose that $\psi(r, \theta, \phi, t)$ is a function describing the displacement of the material from its equilibrium.

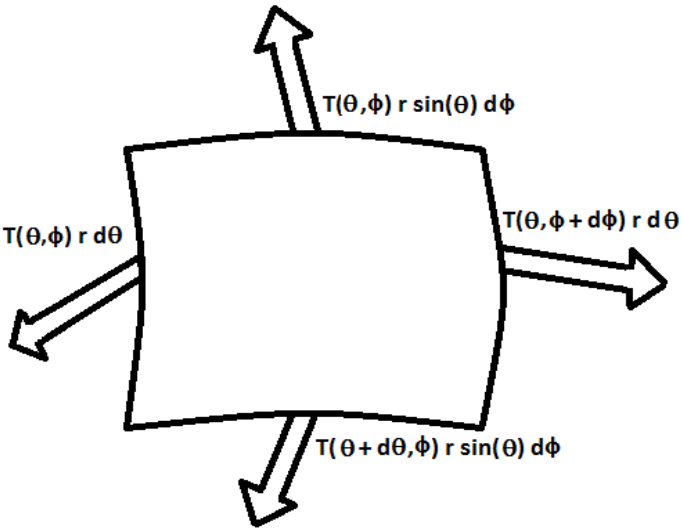

Figure 3: Forces on an area element of a sphere of radius r.

We start by considering the effect of increasing ϕ by $d\phi$. Then the material would move an actual distance of $r \sin\theta d\phi$ on the surface, so our deviation from the

horizontal would be $(1/r)\sin\theta(\partial\psi/\partial\phi)$. Now we can write down the vertical force from tension on the two longitude sides. The downward force from our tension on the longitudinal edge is $Trd\theta\partial\psi(r,\theta,\phi,t)/\partial\phi$, while the upward force is $Trd\theta\partial\psi(r,\theta,\phi+d\phi,t)/\partial\phi$. If we combine these in the usual method, we end up with a contribution to the force, experienced by the volume element, to be

$$dF_{r,\theta} \;=\; Trd\theta d\phi\left(\frac{\partial}{\partial\phi}\right)\frac{1}{r\sin\theta}\left(\frac{\partial\psi}{\partial\phi}\right)\;.$$

Next we need to find the force on the two latitude sides. If we look at the top one first, our slope is $1/r\partial\psi/\partial\theta$. Hence, our force for the top one would be $Tr\sin\theta d\phi(1/r)(\partial\psi/\partial\theta)$. It is important to note that $sin\theta$ varies with θ as well as ψ, so the sum of the forces on this side is

$$dF_{r,\phi} \;=\; Trd\phi d\theta\left(\frac{\partial}{\partial\theta}\right)\sin\theta\left(\frac{1}{r}\right)\left(\frac{\partial\psi}{\partial\theta}\right)\;.$$

As with the other previous derivations of the wave equation, we will now be able to write our equation using Newton's Law ($F=ma$). The mass of the volume element of the material is $\rho\, r^2\sin\theta d\theta d\phi$, where ρ denotes the mass per unit volume. We now have the following expression using the condition that $dF_{r,\theta}+dF_{r,\phi}=dm\cdot a$:

$$\begin{aligned} Trd\theta d\phi\left(\frac{\partial}{\partial\phi}\right)\frac{1}{r\sin\theta}\left(\frac{\partial\psi}{\partial\phi}\right) \quad+\quad Trd\phi d\theta\left(\frac{\partial}{\partial\theta}\right)\sin\theta\left(\frac{1}{r}\right)\left(\frac{\partial\psi}{\partial\theta}\right) \\ = \;\rho r^2\sin\theta d\theta d\phi\left(\frac{\partial^2\psi}{\partial t^2}\right)\;. \end{aligned}$$

Dividing by $d\theta d\phi$ and using the rules of partial derivatives, gives

$$\begin{aligned} & T\left(\frac{\partial}{\partial\phi}\right)\frac{1}{\sin\theta}\left(\frac{\partial\psi}{\partial\phi}\right)\;+\;T\left(\frac{\partial}{\partial\theta}\right)\sin\theta\left(\frac{\partial\psi}{\partial\theta}\right) \quad=\quad \rho r^2\sin\theta\left(\frac{\partial^2\psi}{\partial t^2}\right) \\ \Rightarrow\qquad & T\frac{1}{\sin^2\theta}\left(\frac{\partial^2\psi}{\partial\phi^2}\right)\;+\;T\frac{1}{\sin\theta}\left(\frac{\partial}{\partial\theta}\right)\sin\theta\left(\frac{\partial\psi}{\partial\theta}\right) \quad=\quad \rho r^2\left(\frac{\partial^2\psi}{\partial t^2}\right) \\ \Rightarrow\qquad & \frac{1}{\sin^2\theta}\left(\frac{\partial^2\psi}{\partial\phi^2}\right)\;+\;\frac{1}{\sin\theta}\left(\frac{\partial}{\partial\theta}\right)\sin\theta\left(\frac{\partial\psi}{\partial\theta}\right) \quad=\quad \frac{r^2}{v^2}\left(\frac{\partial^2\psi}{\partial t^2}\right)\;, \end{aligned}$$

where $v=\sqrt{T/\rho}$. Converting the above wave equation into Cartesian coordinates

yields another form of the wave equation, and in all actuality is the one that will be referenced when necessary in the remainder of the text:

$$\frac{\partial^2 \psi}{\partial t^2} \;=\; v^2 \left(\frac{\partial^2 \psi}{\partial x^2} \;+\; \frac{\partial^2 \psi}{\partial y^2} \;+\; \frac{\partial^2 \psi}{\partial z^2} \right)_{r=constant} \;.$$

This equation is analogous to the one stated in the introduction but has the somewhat different expression:

$$\Delta_{S^2}\, \psi \;=\; \frac{r^2}{v^2}\, \frac{\partial^2 \psi}{\partial t^2} \;,$$

where Δ_{S^2} is the Laplace-Beltrami operator on the unit sphere S^2 in $\mathbb{R}^3$, defined to be

$$S^2 \;=\; \left\{ (x, y, z) \in \mathbb{R}^3 \mid x^2 + y^2 + z^2 \;=\; 1 \right\} \;.$$

For ocean waves that travel on the surface of the earth, it is reasonable to take the radial distance from the center r to be a constant.

2.4 Non-linear water wave equations

In this section we examine the equations that govern the motion of the surface of a large body of water. A necessary equation for our designs here is the Korteweg-De Vries, or KdV, equation. Traveling waves that are the solutions of this equation, have been of some interest for over 150 years. It all started with a Scottish engineer named John Scott Russell and his observations of a mass of water pushed through a channel by a boat [7]. This mass of water did not follow the models of the results of the standard differential equations used to represent traveling waves. The mass of water in question is what we call a **soliton**; a soliton is a solitary wave. A paper was published in 1895 that contained an equation that described small-amplitude long-wavelength waves on the surface of water [7]. This paper was submitted by

Diederik Korteweg and Gustav de Vries, who had been studying the phenomenon. It wasn't until the mid 1960's, however, that this idea began to be appreciated. Applied scientists began using digital computers to study nonlinear wave propogation around this time. This paper will contain a derivation of the KdV equation.

We begin with the conservation equations, per unit volume, for fluid motion:

$$\text{Conservation of Mass:} \quad \partial_t \rho + \nabla \cdot (\rho \vec{v}) = 0 \quad , \tag{2.8}$$

$$\text{Conservation of Momentum:} \quad \rho(\partial_t + \vec{v} \cdot \nabla)\vec{v} = -\nabla P + \vec{f} \quad . \tag{2.9}$$

where ρ is the density and $\vec{v}$ is the velocity of the fluid, P is the internal pressure of the fluid and $\vec{f}$ is the external force per unit volume in $\mathbb{R}^3$. We have defined the gradient earlier. If we assume our fluid is both irrotational and incompressible, we are given additional constraints:

$$\text{Irrotational Flow:} \quad \nabla \times \vec{v} = \vec{0} \quad , \tag{2.10}$$

$$\text{Incompressibility:} \quad \nabla\rho = 0 \ , \quad \partial_t \rho = 0 \quad . \tag{2.11}$$

We now analyze these conditions. The statement in (2.10) means there are no vortices in the fluid. Thus the curl, which is related to the rotation or angular momentum of a velocity field, is zero. The statements in (2.11) mean that its volume is not changed by an increase or decrease in pressure. As a result, the density of the fluid does not change. Hence $\partial_x \rho = 0$, $\partial_y \rho = 0$, $\partial_z \rho = 0$ and $\partial_t \rho = 0$.

The irrotationality condition (2.10) is of particular significance since it implies that the velocity $\vec{v}$ can be expressed in terms of a **velocity potential** ϕ, so that

$$\vec{v} = u\,\hat{x} + v\,\hat{y} + w\,\hat{z} = \begin{pmatrix} u \\ v \\ w \end{pmatrix} = \begin{pmatrix} \partial_x \phi \\ \partial_y \phi \\ \partial_z \phi \end{pmatrix} = \nabla\phi \ . \tag{2.12}$$

From Calculus [12], we know this potential must exist since its curl vanishes as a

result of being irrotational. This potential will satisfy Laplace's equation,

$$\Delta\phi \;\equiv\; \nabla^2\phi \;=\; 0\;, \tag{2.13}$$

where Δ is the Laplace operator on $\mathbb{R}^3$. These will be inserted into the first of our hydrodynamic equations. With this, equations (2.8) and (2.9) still have to be satisfied. If we consider the case where the external force is caused by gravity, we set

$$\vec{f} \;=\; -\rho\, g\, \hat{z} \;=\; -\begin{pmatrix} 0 \\ 0 \\ \rho\, g \end{pmatrix}\;,\quad \hat{z} \;\equiv\; \begin{pmatrix} 0 \\ 0 \\ 1 \end{pmatrix}\;,$$

which is the force per unit volume due to gravity. Now we can use a triple vector identity, as the fluid was assumed to be irrotational:

$$\vec{v}\times(\nabla\times\vec{v}) \;=\; -(\vec{v}\cdot\nabla)\,\vec{v} \;+\; \frac{1}{2}\nabla(\vec{v})^2\;.$$

In order to verify this identity, we need the product rule for a gradient multiplying to the dot product of two vectors:

$$\nabla(A\cdot B) \;=\; (A\cdot\nabla)B + (B\cdot\nabla)A + A\times(\nabla\times B) + B\times(\nabla\times A).$$

When $A = B$, we have

$$\begin{aligned}
& \nabla(A\cdot A) &&= (A\cdot\nabla)A + (A\cdot\nabla)A + A\times(\nabla\times A) + A\times(\nabla\times A) \\
\Rightarrow\quad & \nabla(A\cdot A) &&= 2(A\cdot\nabla)A + 2A\times(\nabla\times A) \\
\Rightarrow\quad & 2A\times(\nabla\times A) &&= \nabla(A\cdot A) - 2(A\cdot\nabla)A \\
\Rightarrow\quad & A\times(\nabla\times A) &&= -(A\cdot\nabla)A + \frac{1}{2}\nabla(A\cdot A)\;.
\end{aligned}$$

When $A = \vec{v}$, we get our 3-vector identity, where $(\vec{v})^2 = \vec{v}\cdot\vec{v}$. We already mentioned that $\nabla\times\vec{v} = \vec{0}$, as our fluid is irrotational; this allows us to simplify our 3-vector

identity as such:

$$\begin{aligned} \vec{v} \times (\nabla \times \vec{v}) &= -(\vec{v} \cdot \nabla)\vec{v} + \frac{1}{2}\nabla(\vec{v})^2 \\ \Rightarrow \qquad \vec{v} \times \vec{0} &= -(\vec{v} \cdot \nabla)\vec{v} + \frac{1}{2}\nabla(\vec{v})^2 \\ \Rightarrow \qquad 0 &= (\vec{v} \cdot \nabla)\vec{v} + \frac{1}{2}\nabla(\vec{v})^2, \qquad \text{as } \vec{v} \times \vec{0} = \vec{0} \ , \end{aligned}$$

which, due to Eq.(2.12), can be written as,

$$(\vec{v} \cdot \nabla)\vec{v} \ = \ \frac{1}{2}\nabla(\vec{v})^2 \ = \ \nabla\left((u^2 + v^2 + w^2)/2\right) \ . \tag{2.14}$$

Now, since $\vec{v} = \nabla\phi$, equation (2.9) becomes:

$$\partial_t \nabla\phi + (\vec{v} \cdot \nabla)\ \vec{v} \ = \ -\nabla\frac{P}{\rho} + \frac{\vec{f}}{\rho} \ .$$

Substituting the triple vector identity into Eq.(2.14) and recalling $\vec{f} = -\rho g\hat{z}$ yields:

$$\partial_t \nabla\phi + \frac{1}{2}\nabla(\vec{v})^2 + \nabla\frac{P}{\rho} + g\hat{z} \ = \ 0 \ .$$

Finally, the simple fact that $\nabla z = \hat{z}$ allows us to factor out the ∇ operator to obtain

$$\nabla\left(\partial_t\phi + \frac{1}{2}(\vec{v})^2 + \frac{P}{\rho} + gz\right) \ = \ 0 \ . \tag{2.15}$$

Observe that the quantity under ∇ must depend solely on time. Integrating Eq.(2.15) gives an arbitrary constant that can be absorbed into the pressure term. Indeed, the quantity P/ρ is a type of potential energy, so adding a constant term to it will not affect its role in determining the velocities. Thus we conclude with the equation

$$\partial_t\phi \ + \ (u^2 + v^2 + w^2)/2 \ + \ P/\rho \ + \ gz \ = \ 0 \ , \tag{2.16}$$

Summing up, we now have two non-linear coupled partial differential equations for determining velocities;

$$\Delta\phi = 0\ , \tag{2.17}$$

$$\partial_t\phi + \frac{1}{2}(\nabla\phi)^2 + \frac{P}{\rho} + gz = 0. \tag{2.18}$$

In general these equations are very difficult to solve for $\phi(x, y, z, t)$. To attempt a solution, the quatities ρ, P and g must be known, and initial conditions, along with any boundary conditions, must be specified.

2.5 KdV equation for 1-D Channel Flow

We are interested in the flow of the water down a long channel which is narrow enough to be considered one-dimensional. Remember, the water here is both incompressible and irrotational. Now we can set up an $\hat{x}$-axis along the length of the channel and a $\hat{z}$-axis vertically; the nature of our assumptions allows us to ignore the $\hat{y}$ direction. We will assign h to the value of the depth of the water at rest; a characteristic length of the waves to be searched for is given by l, called the wavelength, and we assume $l \gg h$. On the other hand, we still want our flow to be irrotational; as such, we want to avoid any turbulence in motion. Let us have a well–a cavity in which we can contain a liquid–to restrain the waves we are searching for. Now we can assign the constant a to their maximum amplitude, and we want $a \ll h$.

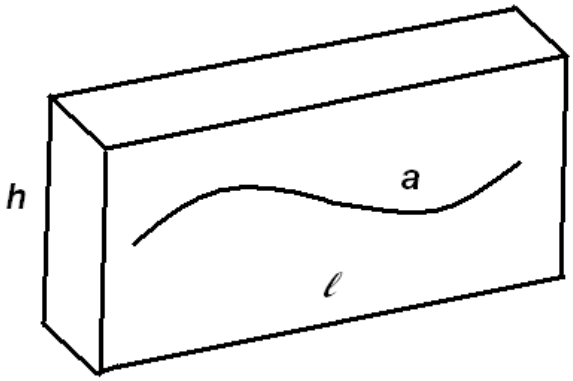

Figure 4: Relative sizes of parameters $\ell \gg h > a > 0$.

Thus we can define a pair of variables to the quantities created by these requirements:

$$\epsilon = \frac{a}{h}, \qquad \delta = \left(\frac{h}{l}\right)^2$$

For example, if the depth $h = 1000$ m, then $l \approx 1000$ km and $a \approx 1$ m. Note that both of these values will be small. Now, suppose the surface of the water at rest corresponds to $z = h$ (the zero for the vertical direction), and that we take the pressure to vanish at (and near) the surface. Since the bottom is fixed in such a way that the water cannot move it, we are able to use it as a boundary. Hence we have the following boundary condition:

$$(\vec{v})_z|_{bottom} \;=\; v|_{bottom} = \frac{\partial \phi}{\partial z}(x, 0) = 0 \tag{2.19}$$

Let us define as our variable amplitude of the traveling waves $\eta = \eta(x, t)$, where $|\eta| \leq a$, so that the surface of the fluid with waves traveling on it will be given by

$$\begin{aligned} z|_{surface} &= h \;+\; \eta(x,t) \qquad (2.20)\\ \Rightarrow \qquad v|_{surface} &= \frac{dz}{dt}|_{surface} \;=\; \partial_t \eta \;+\; \partial_x \eta \, \frac{dx}{dt}|_{surface} \\ \Rightarrow \qquad \phi_z|_{surface} &= \partial_t \eta \;+\; \phi_x|_{surface} \, \partial_x \eta \end{aligned}$$

Now recall that pressure vanishes at the surface. This allows us to simplify the equation (2.18) with the triple vector identity, equation (2.14), plugged in. We can simplify it at the surface now. Recall that u and w are coefficients of $\vec{v}$, ignoring the $\hat{y}$ coefficient, ie. $v = 0$:

$$\partial_t\phi + \frac{1}{2}(\nabla\phi)^2 + \frac{P}{\rho} + gz \;=\; \partial_t\phi + \frac{1}{2}(u^2 + w^2) + \frac{P}{\rho} + gz \;=\; 0$$

and since the pressure vanishes at the surface,

$$\phi_t|_{surface} \;+\; \frac{1}{2}(u^2 + w^2)|_{surface} \;+\; g\eta \;=\; 0\ . \tag{2.21}$$

Now consider the above equations for the following conditions:

$$\nabla^2\phi = 0,\ \phi_z(x, z = -h) = 0 \quad \text{(very small amplitude)}$$
$$\partial_t\eta - \partial_z\phi = 0 \quad \text{(at the surface)}$$
$$\partial_t\phi + g\eta = 0 \quad \text{(at the surface)} \tag{2.22}$$

We can eliminate the wave amplitude function η from all but equation (2.22) by differentiating and substituting:

$$\frac{\partial}{\partial t}(\partial_t\phi + g\eta) = \partial_{tt}\phi + g\partial_t\eta = \partial_{tt}\phi + g\partial_z\phi, \quad \text{as} \quad \partial_t\eta = \partial_z\phi \tag{2.23}$$

Now when we can find a potential ϕ in (2.23), this last equation allows us to solve for η. Now, we know we are interested in some sort of a wavelike solution. To that end, let us attempt something from a differential equations class: assume a solution and see if it works. Let's say for ϕ we have the sinusoidal function

$$\phi = Z(z) \cdot \sin(kx - \omega t) \tag{2.24}$$

The requirements from our Laplace equation, (2.13), necessitate that

$$Z(z) \;=\; Ae^{kz} \;+\; Be^{-kz}\;.$$

When this is inserted into equation (2.19), we get this:

$$v|_{bottom} = \frac{\partial\phi}{\partial z}(x,0) \;=\; \frac{\partial}{\partial z}(Ae^{kz} + Be^{-kz})\cdot\sin(kx) \;=\; 0$$

$$\Rightarrow \qquad Ake^{kz}\sin(kx) \;-\; Bke^{-kz}\sin(kx) \;=\; 0$$

$$\Rightarrow \qquad Ake^{kz}\sin(kx) \;=\; Bke^{-kz}\sin(kx)$$

$$\Rightarrow \qquad A\frac{ke^{kz}\sin(kx)}{ke^{-kz}\sin(kx)} \;=\; B$$

$$\Rightarrow \qquad \frac{B}{A} \;=\; e^{2kz}\;.$$

But, recalling that at $t = 0$, $z = h$, we conclude that

$$\frac{B}{A} = e^{-2kh},$$

which, when substituted into (2.24) yields:

$$\phi(x,y,z,t) \;=\; 2Ae^{kh}\cosh[k(z+h)]\sin(kx-\omega t) \tag{2.25}$$

Substituting this result into equation (2.23) yields:

$$\partial_{tt}(2Ae^{kh}\cosh(kz+kh)\sin(kx-\omega t)) + g\partial_z(2Ae^{kh}\cosh(kz+kh)\sin(kx-\omega t)) \;=\; 0$$

$$\Rightarrow \quad -2A\omega^2 e^{kh}\cosh(kz+kh)\sin(kx-\omega t) + 2gkAe^{kh}\sinh(kz+kh)\sin(kx-\omega t) = 0$$

$$\Rightarrow \quad 2A\omega^2 e^{kh}\cosh(kz+kh)\sin(kx-\omega t) \;=\; 2gkAe^{kh}\sinh(kz+kh)\sin(kx-\omega t)$$

$$\Rightarrow \quad \omega^2 \;=\; gk\frac{\sinh(kz+kh)}{\cosh(kz+kh)}$$

This gives us an equation for the frequency:

$$\omega^2 \;=\; gk\,\tanh(kz+kh)|_{surface} \;=\; gk\,\tanh(kh)\;. \tag{2.26}$$

This allows us to determine our wave amplitude:

$$\eta(x,t) \;=\; (1/g)\;\phi_t \;=\; A\,\sqrt{(2k/g)\sinh(2kh)}\sin(kx-\omega t)\;.$$

As we can see here, our wave has an amplitude that is dependent on the wavelength. Additionally, our wave has a dispersion relation for its frequency saying that ω is directly proportional to k with something between them. In effect, this factor is the speed v_0 where $v_0 \equiv \sqrt{gh}$ when k is near 0 (very long wavelength) but is more like $\sqrt{g/k} = v_0/\sqrt{kh} = 2\pi v_0\sqrt{\lambda/h}$ as the wavelength shortens, where $\lambda = kh^2/(4\pi^2)$. This tells us what it means for the wavelength to be longer or shorter; the important factor is the ratio of the wavelength to the depth of the channel. Moreover, waves with longer wavelength travel faster and with less dispersion than shorter wavelength waves.

Now we can move forward to look at higher levels of disruption. If we differentiate equation (2.18) along the channel (in effect, with respect to x), and evaluating it at the surface, we end up with the following for the velocity potential:

$$\phi_{xt} + \frac{1}{2}(2)(\phi_x\phi_{xx} + \phi_z\phi_{xz}) + g\eta_x \;=\; u_t + uu_x + vv_x + g\eta_x \;=\; 0\;.$$

A standard sort of approach to small amplitude deviations is to expand ϕ into a power series of the height variable z. If we were to expand ϕ into such a power series, we would end up with the following:

$$\phi(x,z,t) \;=\; \sum_{0}^{\infty} z^n \phi_n(x,t) \;.$$

Now, taking the partial derivative wrt z gives,

$$\phi_z \;=\; \sum_{0}^{\infty} n z^{n-1} \phi_n \;=\; 0 + \sum_{1}^{\infty} n z^{n-1} \phi_n \;=\; \sum_{1}^{\infty} n z^{n-1} \phi_n \;.$$

From equation (2.19) we have

$$\phi_1 = 0,$$

a very important result. Hence, inserting into Laplace's equation $\Delta\phi = 0$ yields:

$$\sum_{0}^{\infty} z^n [\phi_{n,xx} + (n+2)(n+1)\phi_{n+2}] = 0 \qquad \Rightarrow \qquad \phi_{n,xx} + (n+2)(n+1)\phi_{n+2} = 0 \;,$$

which establishes a recursion relationship for each $n\mathbb{N}$ among the coefficients!

Now, with $\phi_1 = 0$, all of the odd terms of the series must vanish. Thus we are able to simplify ϕ to:

$$\phi(x,z,t) \;=\; \sum_{0}^{\infty} \frac{(-1)^m z^{2m}}{(2m)!} \alpha^{2m},$$

where $\alpha \equiv \phi_0(x,t)$. Now we can say:

$$\Rightarrow \qquad \left\{ \begin{array}{l} u = \phi_x \;=\; \alpha_x - \frac{1}{2!} z^2 \alpha_{xxx} + \frac{1}{4!} z^4 \alpha_{xxxxx} + ... \\ w = \phi_z \;=\; -z\alpha_{xx} + \frac{1}{3!} z^3 \alpha_{xxxx} - \frac{1}{5!} z^5 \alpha_{xxxxxx} + ... \end{array} \right.$$

where the notation α^{2m} refers to the $(2m)^{th}$ derivative of α with respect to x.

At this point, we are dealing with a nonlinear problem. It'd be useful for us to instantiate some new, dimensionless variables so we can introduce quantities of small order already mentioned. For example, we will use l for the characteristic length to which we will scale the horizontal distance. Our time will be scaled to the simplest linear speed of the v_0's from earlier, namely $v_0 = \sqrt{gh}$, and amplitude in terms of its maximum a. Recall that our potential has such dimensions that its derivative with respect to either x or y should be a velocity. Observe:

$$\bar{x} \equiv x/l, \;\; \bar{z} \equiv z/h, \;\; \bar{t} \equiv t/(l/v_0)$$
$$\bar{\eta} \equiv \eta/a, \;\; \bar{\phi} \equiv h\phi/(alv_0) = \phi/(\epsilon l v_0), \;\; \epsilon = a/h.$$

Now we can see that the surface will be at $\bar{z} = 1 + \epsilon\bar{\eta}$. As a result, we have:

$$\Rightarrow \begin{cases} \bar{u} = u/\epsilon v_0 \\ \bar{w} = (\delta/\epsilon v_0)\; w \\ \bar{\alpha} = \alpha/\epsilon l v_0 \end{cases}$$

It is useful to write out the equations for the dimensionless velocity components first. It helps to have them written from lowest to highest order; for instance, ϵ and δ are of the same order. We introduce the symbol O^n to denote terms of n^{th} order in these quantites. For instance, terms of second order would fall under the blanket of O^2, and would contain anything attached to a term of ϵ^2, δ^2, or $\epsilon\delta$.

$$\bar{\phi} = \bar{\alpha} - \frac{1}{2}(1+\epsilon\eta)^2\delta\bar{\alpha}_{\bar{x}\bar{x}} + O^2$$

$$\bar{u} = \bar{\alpha}_{\bar{x}} - \frac{1}{2}\delta\bar{\alpha}_{\bar{x}\bar{x}\bar{x}} + O^2$$

$$\bar{w} = -\delta[(1+\epsilon\bar{\eta})\bar{\alpha}_{\bar{x}\bar{x}} - \frac{1}{6}\delta\bar{\alpha}_{\bar{x}\bar{x}\bar{x}\bar{x}} + O^2]$$

We can now rewrite our vertical constraints from equation (2.20) with our dimensionless variables, yielding the following results:

$$\bar{z}|_{surface} = 1 + \epsilon\bar{\eta}$$

$$\bar{\phi}_{\bar{z}}|_{surface} = \delta\bar{\eta}_{\bar{t}} + \delta\epsilon\bar{\phi}_{\bar{x}}\bar{\eta}_{\bar{x}}.$$

We also discussed series expansions previously. When these are applied to the quantities we have here, we get:

$$\bar{\eta} + \epsilon\bar{\eta}_{\bar{x}}\bar{\alpha}_{\bar{x}} + (1 + \epsilon\bar{\eta})\bar{\alpha}_{\overline{xx}} - \frac{1}{6}\delta\bar{\alpha}_{\overline{xxxx}} + O^2 = 0. \tag{2.27}$$

Using our other boundary condition from (2.21) yields

$$\bar{\phi}_{\bar{t}} + \frac{1}{2}\epsilon[(\bar{\phi}_{\bar{z}})^2 + (\bar{\phi}_{\bar{x}})^2/\delta] + \bar{\eta} \;=\; 0$$

Again, we will utilize our series expansions here to produce:

$$\bar{\alpha}_{\bar{t}} - \frac{1}{2}[\delta\bar{\alpha}_{\overline{xxt}} + \epsilon(\bar{\alpha}_{\bar{x}})^2] + \bar{\eta} + O^2 \;=\; 0\ . \tag{2.28}$$

Since we are now looking at dimensionless variables, we need to once again evaluate how the equation changes along the channel. To that end, we differentiate our equation with respect to x. Hence we are going to define yet another new variable, say $\omega \equiv \bar{\alpha}_{\bar{x}}$. As an added bonus, we can start writing our variables without the bars. If we do need to convert them back, we have the equivalence relations above to get that done. Differentiating (2.28) by x and replacing α_x with β:

$$\frac{\partial}{\partial x}[\alpha_t - \frac{1}{2}\delta\alpha_{xxt} + \frac{1}{2}\epsilon(\alpha_x)^2 + \eta + O^2 = 0]$$

$$\Rightarrow \alpha_{xt} - \frac{1}{2}\delta\alpha_{xxxt} + (2)\frac{1}{2}\epsilon(\alpha_x)(\alpha_{xx}) + \eta_x = 0$$

$$\Rightarrow \beta_t - \frac{1}{2}\delta\beta_{xxt} + \epsilon\beta\beta_x + \eta_x = 0 \tag{2.29}$$

and taking equation (2.27) allows for:

$$\eta_t + \epsilon\eta_x\alpha_x + (1+\epsilon\eta)\alpha_{xx} - \frac{1}{6}\delta\alpha_{xxxx} + O^2 = 0$$

$$\Rightarrow \eta_t + \epsilon\eta_x\beta + (1+\epsilon\eta)\beta_x + \frac{1}{6}\delta\beta_{xxx} = 0 \tag{2.30}$$

Notice that we didn't write that these equations are correct only to second order. We don't need to anymore. However, it'd be nice if we could clean these up a bit. They do look a touch complicated. Let's make sure these equations are satisfied to zero-th order; that is, for equations that have no ϵ or δ. Therefore, ignoring both the ϵ and δ-terms, we get to reduce our equations. Beginning with (2.30):

$$\eta_t + \beta_x = 0 \tag{2.31}$$

and for (2.29):

$$\beta_t + \eta_x = 0. \tag{2.32}$$

Now, as both of these equations equal zero, we can set them equal to each other.

$$\eta_t + \beta_x = \beta_t + \eta_x$$

Now, separating the unknown functions in these equations implies that

$$\beta_{tt} = \beta_{xx} \qquad and \qquad \eta_{xx} = \eta_{tt} \tag{2.33}$$

This tells us that at the lowest order, both β and η necessarily satisfy wave equations with a speed of 1. Now, β and η seem fairly similar. Their difference may be somewhere in, say, first-order terms. Thus we can assume that a solution exists for ω in terms of η plus some small terms:

$$\beta \equiv \eta + \epsilon \cdot F + \delta \cdot G + O^2 \tag{2.34}$$

for some $F(x,t)$ and $G(x,t)$. We know the physical meanings of ϵ and δ are different, but they have the same approximate size. But since they have different meanings, we write an additional first-order term for the difference. We still need to satisfy equations (2.31), (2.32), and (2.33). Say we plug our assumed solution into (2.31) and (2.32). We get:

$$\eta_t + \epsilon F_t + \delta G_t + \eta_x = 0 = \eta_x + \epsilon F_x + \delta G_x + \eta_t,$$

which implies $\eta_x + \eta_t$ is of first order in ϵ and δ. It also shows us that to lowest order we need $\beta_x + \beta_t$ to vanish. As such, we must impose on our new functions (F and G) the following property:

$$F_x + F_t = O^1, \text{ and } G_x + G_t = O^1$$

Now we can plug these into equations (2.29) and (2.30) with the goal of determining F and G:

$$\beta_t - \tfrac{1}{2}\delta\beta_{xxt} + \epsilon\beta\beta_x + \eta_x = 0$$
$$\eta_t + \epsilon\eta_x\beta + (1+\epsilon\eta)\beta_x + \tfrac{1}{6}\delta\beta_{xxx} = 0$$
$$\Downarrow$$
$$\eta_t + \epsilon F_t + \delta G_t - \tfrac{1}{2}\delta\eta_{xxt} + \epsilon\eta\eta_x + \eta_x = 0$$

$$\eta_t + \epsilon\eta\eta_x + \eta_x + \epsilon F_x \delta G_x + \epsilon\eta\eta_x - \tfrac{1}{6}\delta\eta_{xxx}$$
$$\Downarrow$$
$$\eta_t + \eta_x + \epsilon(F_t + \eta\eta_x) + \delta(G_t - \tfrac{1}{2}\eta_{xxt}) = 0$$
$$\eta_t + \eta_x + \epsilon(F_x + 2\eta\eta_x) + \delta(G_x - \tfrac{1}{6}\eta_{xxx}) = 0.$$

Now utilizing the techniques of solving a system of equations, we will subtract these two equations in order to solve for F and G. From that, we get

$$\epsilon(F_x - F_t - \eta\eta_x + 2\eta\eta_x) + \delta(G_x - G_t + \frac{1}{2}\eta_{xxt} - \frac{1}{6}\eta_{xxx}) = 0$$

$$\Rightarrow F_x - F_t + \eta\eta_x = 0 \quad \text{and} \quad G_x - G_t - \tfrac{2}{3}\eta_{xxx} = 0$$
$$\Rightarrow 2F_x = -\eta\eta_x = -\tfrac{1}{2}(\eta^2)_x, \quad \text{and} \quad 2G_x = \tfrac{2}{3}\eta_{xxx}$$

as $F_x = -F_t$ and $G_x = -G_t$. This implies

$$F_x = -\tfrac{1}{4}(\eta^2)_x, \quad \text{and} \quad G_x = \tfrac{1}{3}\eta_{xxx}$$
$$\Rightarrow \int F_x dx = \int -\tfrac{1}{4}(\eta^2)_x dx, \quad \text{and} \quad \int G_x dx = \int \tfrac{1}{3}\eta_{xxx} dx$$
$$\Rightarrow F = -\tfrac{1}{4}\eta^2, \quad \text{and} \quad G = \tfrac{1}{3}\eta_{xx}$$
$$\Rightarrow \omega = \eta - \tfrac{1}{4}\epsilon\eta^2 + \tfrac{1}{3}\delta\eta_{xx} + O^2$$

Now if you plug this into either of the equations from the system we just solved, we get the following equation:

$$\eta_t + \eta_x + \frac{3\,\epsilon}{2}\,\eta\,\eta_x + \frac{\delta}{6}\,\eta_{xxx} = 0. \tag{2.35}$$

This is one form of the KdV equation. It shows that the nonlinearity (ϵ term) and dispersion (δ term) are small corrections to the 1-D wave equation.

2.6 Modified KdV Equation for 2-D Water Waves

As it turns out, we cannot always rely on the KdV to model our solitons. Sometimes circumstances are such that the KdV no longer fits, as it is. For this, we need a KdV that works for a two-dimensional case. However, to produce an equation that is predominately a balance between weak dispersion and weak non-linearity in the direction of propogation and is two dimensional, we need to assume a nearly-plane wave. For this, we will use a two-dimensional case of the KdV equation. Now, say our KdV equation is as follows:

$$\eta_t + \eta_x + \frac{3\epsilon}{2}\eta\eta_x + \frac{\delta}{6}\eta_{xxx} \;=\; f \;, \tag{2.36}$$

where f is some forcing on the KdV. For this, we choose $f(x, y, t)$ as a solution of

$$f_x \;=\; -v(x, y) \cdot \eta_{yy} \;, \tag{2.37}$$

for our y-coupling equation [7]. This provides a way to program the 2-D KdV; using a leapfrog method. The numerical approach involves solving for f using η in (2.37). Then η is solved using equation (2.36) now that f has been obtained, etc.

A single nonlinear PDE can be obtained by differentiating both sides of (2.36) and using (2.37) to give

$$\left(2\eta_t \;+\; v \cdot \eta_x \;+\; 3\eta\eta_x \;+\; \frac{1}{3}\eta_{xxx}\right)_x \;+\; v \cdot \eta_{yy} \;=\; 0 \;,$$

which extend the KdV to 2-D surface waves. This allows us to model more complex soliton propogation and runup. In our model of the North Carolina coast in a later chapter, we will see this equation have a great deal of value to our research.

CHAPTER 3: Wavelet basics

The various wavelet types used in this thesis are discussed in detail in the class handouts from the graduate level Numerical Analysis course.

Consider the functions $f : \mathbb{R} \to \mathbb{R}$ to be actually observed entities. We will say

$$f \in \mathcal{L}^p \iff \int_{-\infty}^{\infty} |f(x)|^p dx < \infty, p \geq 1 \ ,$$

$$f \in \mathcal{L}^\infty \iff sup_{x \in \mathbb{R}} |f(x)| < \infty \ ,$$

Now, the $\mathcal{L}^p$ norm of a function f is defined as

$$||f||_p = \left(\int_{-\infty}^{\infty} |f(x)|^p dx \right)^{1/p}, \qquad ||f(x)||_\infty = \sup_{x \in \mathbb{R}} |f(x)| \ .$$

For our next observation, we will need to know what a Cauchy sequence is. So, for a sequence $\{x_n\}$ to be Cauchy, we must have:

$$\forall \epsilon > 0 \in \mathbb{R} \ \exists \ N \in \mathbb{N} \ni \forall m, n \in \mathbb{N}, \ m, n > N \Rightarrow |x_n - x_m| < \epsilon \ .$$

We observe that the completion of $\mathcal{L}^p$ under Cauchy sequences in the $\mathcal{L}^p$ norm is a Banach space. The case that $p = 2$ is special, because we can define an inner product

$$\forall f, g \in \mathcal{L}^2 < f, g >= \int_{-\infty}^{\infty} f(x) \cdot g(x) dx \ .$$

Then $f \perp g$, i.e. f is orthogonal to g, iff $< f, g >= 0$. Thus,

$$||f||_2 = \sqrt{< f, f >}$$

Now, a little more about $\mathcal{L}^2$. $\mathcal{L}^2$ is a Hilbert space, which is a closed Euclidean space. But what exactly do we mean by that? Well, a Hilbert space is a vector space H with an inner product $< f, g >$ such that the norm defined by $||f|| = \sqrt{< f, f >}$ turns H into a complete metric space; that is, a metric space in which every Cauchy sequence is convergent. As it turns out, $\mathcal{L}^2$ has many properties:

$| < f, g > | \leq ||f||_2 ||g||_2$ (Cauchy-Schwarz inequality)

$af + bg \in \mathcal{L}^2$ if $a, b \in \mathbb{R}$ and $f, g \in \mathcal{L}^2$ (Linearly closed)

$||f + g||_p \leq ||f||_p + ||g||_p$ (Triangle inequality)

$\exists \{\Psi_k\}_{k=1}^{\infty} \subset \mathcal{L}^2$ so that

1) $||\Psi_x||_2 = 1$

2) $\Psi_k \perp \Psi_j$ for $k \neq j$

3) $\overline{span\{\Psi_k\}} = \mathcal{L}^2$.

Thus, $\mathcal{L}^2$ has an orthogonal basis, which is countable. We refer to this as a Separable Hilbert Space. The first published basis of $\mathcal{L}^2$ was by Haar in 1910. Back then, it was not called a wavelet; this has only happened within the past 30-40 years. If we define what we call the Mother Wavelet Function as

$$h(x) = \begin{cases} -1/\sqrt{2}, & 0 < x < 1 \\ 1/\sqrt{2}, & 1 < x < 2 \\ 0, & otherwise, \end{cases}$$

then we can define the wavelet basis frame as

$$\Lambda^h \equiv \{h_{j,k}(x) = 2^{j/2} h(2^j x - k) \mid j, k \in \mathbb{Z}\}. \tag{3.1}$$

Note that if we set $j = 0$, $k = 0$ we end up with

$$h_{0,0}(x) \equiv 2^{0/2} h(2^0 x - 0) = h(x)$$

Now, any function $f \in \mathcal{L}^2$ can be expressed as a linear combination from (3.1). As such, $\exists\{C_{j,k}\}, j, k \in \mathbb{Z}$ so that

$$f(x) = \sum_{j=-\infty}^{\infty} \sum_{k=-\infty}^{\infty} C_{j,k} h_{j,k}(x)$$

In order to find the coefficients of the wavelet expansion, notice the inner product $< h_{j,k}, h_{j',k'} >= \delta_{j,j'}\delta_{k,k'}$, where $\delta_{i,j}$ denotes the Kronecker Delta function

$$\delta_{i,j} = \begin{cases} 1, & j = j' \\ 0, & j \neq j' \end{cases}$$

Thus, multiplying the expression for $f(x)$ on the right by $h_{j',k'}(x)$ and integrating on $\mathbb{R}$ yields

$$\int_{-\infty}^{\infty} f(x) h_{j',k'}(x) = \int_{-\infty}^{\infty} \sum_{j} \sum_{k} C_{j,k} h_{j,k}(x) h_{j',k'}(x) dx$$

$$\Rightarrow < f, h_{j',k'} >= \sum_{j,k} C_{j,k} < h_{j,k}, h_{j',k'} >= C_{j',k'}$$

This gives the Haar wavelet transform of the function $f \in \mathcal{L}^2(\mathbb{R})$ to the infinite sequence of constant coefficients $\{C_{j,k}\} \in l^2(\mathbb{Z}^2)$. We will now describe how the filtering process proceeds through a wavelet transform. Say we have a function $f \in \mathcal{L}^2$. We send it through a wavelet transform (this is the analysis step) and get l^2 (discrete form of $\mathcal{L}^2$) coefficients $\{C_{j,k}\}$. Then we sort out the coefficients, yielding $\{C_{J(l),K(l)}\}, l \in \mathbb{N}$ with $|C_{J(l),K(l)}| \geq |C_{J(l+1),K(l+1)}|$. Now in order to filter them, set $C_{J(l),K(l)} = 0$ for $l \geq L \in \mathbb{N}$. This enables us to rebuild an approximation of our function as a finite sum

$$\tilde{f}(x) = \sum_{l=1}^{L} C_{J(l),K(l)} h_{J(l),K(l)}$$

In this way, $\tilde{f}(x)$ is an $\mathcal{L}^2$-approximation of $f(x)$. The size of the difference is measured

by the RMS (Root Mean Square) value

$$dist_2(f, \tilde{f}) = \sqrt{\int_{-\infty}^{\infty} |f(x) - \tilde{f}(x)|^2 dx} = ||f - \tilde{f}||_2$$

The Fourier transform of $f \in \mathcal{L}^2(\mathbb{R})$ is defined to be

$$\hat{f}(\xi) = \mathcal{F}[f](\xi) = \frac{1}{\sqrt{2\pi}} \int_{-\infty}^{\infty} e^{-ix\xi} f(x) dx$$

The function $f(x)$ is reconstructed from its transform $\hat{f}(\xi)$ using the inverse Fourier transform

$$\mathcal{F}^{-1}[\hat{f}](x) = \frac{1}{\sqrt{2\pi}} \int_{-\infty}^{\infty} e^{ix\xi} \hat{f}(\xi) d\xi$$

This works because of the following:

$$\int_{-\infty}^{\infty} e^{-ix'\xi} e^{ix\xi} d\xi = \int_{-\infty}^{\infty} e^{i(x-x')\xi} d\xi = 2\pi\delta(x - x')$$

where $\delta(x - x')$ is the Dirac Delta function, which satisfies

$$\int_{-\infty}^{\infty} g(x')\delta(x - x') dx' = g(x)$$

As a side note, let's review our discussion of the delta function. $\delta(x - x')$ isn't really a function. It's actually a distribution, and so it only makes sense when used with integration.

Now, a Fourier transform has many properties. It is a linear transformation, and it is unitary on $\mathcal{L}^2$. It being linear means it is operation-preserving with respect to addition and scalar multiplication, while the unitary property refers to the fact that a Fourier transform rotates the function, but does not change its size. As a result,

the $\mathcal{L}^2$ norm of the transformed function equals that of the original function. The properties look like this:

1) $\mathcal{F}[af + bg] = a\mathcal{F}[f] + b\mathcal{F}[g]$ (linearity)

2) $||\hat{f}||_2 = ||\mathcal{F}(f)||_2 = ||f||_2$ (norm-preserving)

The power spectrum of $f \in \mathcal{L}^2$ is the non-negative real function $|\hat{f}(\xi)|^2$. Where the power is large, there will be a frequency ξ in the function f. To measure or detect frequencies in a data set, use the Fast Fourier Transform. This is a way to program a Fourier transform in something like the C++ programming language. Say we have real data in vector form with length 2^N. Once we take the Fast Fourier Transform of the data we have, our result will be complex coefficients in vector form of length $2 \cdot 2^N = 2^{N+1}$.

As with wavelets, the modulus of the coefficients can be sorted, then the list can be chopped or filtered and an approximation constructed. Unfortunately, the reconstruction is often compex-valued, even though the data set was real-valued. Still, Fast Fourier Transforms are useful. As a Fourier transform is a unitary transformation, we have the Plancherel property:

$$< f, h > = < \hat{f}, \hat{h} > ,$$

which shows that the Fourier transform is merely a rotation.

A mother wavelet $\Psi(x)$ is a function with the following properties:

1) $\int_{-\infty}^{\infty} |\Psi(x)|dx = ||\Psi||_1 < \infty$ Ψ is integrable
2) $\int_{-\infty}^{\infty} |\Psi(x)|^2 dx = ||\Psi||_2^2 < \infty$ Ψ is square integrable
3) $\int_{-\infty}^{\infty} \Psi(x)dx = 0$ the average of Ψ is 0
4) $\int_{-\infty}^{\infty} \frac{|\hat{\Psi}(\xi)|^2}{|\xi|} d\xi < 0$ (Ψ is admissible),

where **admissible** means the wavelet transform has an inverse.

Once a mother wavelet $\Psi(x)$ has been found/constructed/designed, two parameters are chosen:

$$a \equiv \text{scale} > 1 \qquad b \equiv \text{shift} > 0 \ .$$

The corresponding wavelet frame is

$$\Lambda_{a,b}^{\Psi} \equiv \{\Psi_{j,k}(x) \equiv a^{j/2}\Psi(a^j x - bk)\}_{j,k\in\mathbb{Z}} \ .$$

For the wavelets we use to analyze both tsunamis and rogue waves, this is a good place to institute some variables. We have mentioned the speed of the wave, which we can also refer to as celerity. We set the function $v(t, x, y)$ as the speed, which is dependent on the acceleration due to gravity (near constant on the earth's surface) and the depth function $H(t, x, y)$. Remember that we said $v_0 \equiv \sqrt{gh}$, so now we want $v^2 = gH$. We will use v_0 as the speed when the ocean floor is constant. Tsunamis and rogue waves are created by a forcing, which we will define as the function $F(t, x, y)$. When we see a forcing, it is expected to be short-lived.

We will also define a few special functions that we will be using throughout this paper. One of the most important is $K_q(t)$, the function which satisfies the Multiplicatively Advanced Differential Equations (MADE) that we use throughout the work. We will set $K_q(t) \equiv 0$ for $t \leq 0$ and define from [8]

$$K_q(t) \equiv \sum_{j=-\infty}^{\infty} (-1)^j e^{q^j t}/q^{j(j+1)/2}, \text{ for } t > 0, \ q > 1$$

K_q is the solution of:

$$K_q'(t) = K_q(qt), \qquad \forall t \in \mathbb{R}, \ q > 1 \ .$$

Now, K_q satisfies the properties of a wavelet, as mentioned above. Furthermore, the reproducing kernel of $K_q(t)$ gives the following functions [9]:

The ${}_qCos$ function from [10]:

$$ {}_qCos(t) = N_q \cdot \int_0^\infty K_q(u)K_q(u-t)du \;=\; N_q \sum_{j=-\infty}^{\infty} (-1)^j e^{-q^{2j|t|}}/q^{j^2} \tag{3.2} $$

And the ${}_qSin$ function from [10]:

$$ {}_qSin(t) = -N_q \cdot \int_0^\infty K_q(u)K_q(qu-qt)du \;=\; \frac{t}{|t|} N_q \sum_{j=-\infty}^{\infty} (-1)^j e^{-q^{2j|t|}}/q^{j(j-1)} \tag{3.3} $$

Here, N_q is a normalizing constant:

$$ N_\epsilon = \int_0^\infty {K_\epsilon}^2 du = {||K_\epsilon||_2}^2 $$

from [10]. Additionally, it can be shown that

$$ {}_qCos''(t) \;=\; -q \cdot {}_qCos(qt), \qquad {}_qSin''(t) \;=\; -q^2 \cdot {}_qSin(qt) \tag{3.4} $$

It is shown in [9] that ${}_qCos(t) \;\to\; cos(t)$ and ${}_qSin(t) \;\to\; sin(t)$ pointwise for $t \in \mathbb{R}$ as $q \;\to\; 1^+$ and uniformly on compact sets. Therefore, ${}_qCos(t)$ and ${}_qSin(t)$ can be viewed as $\mathcal{L}^2$ approximations of $cos(t)$ and $sin(t)$, and we discussed $\mathcal{L}^2$ approximations earlier.

3.1 A one-sided Tsunami-like wavelet

A tsunami is a fast moving, low amplitude wave caused by a forcing event at or near the seabed. To model a tsunami, a one-sided, non-symmetric profile is used. In

modeling these, we utilize the following q-advanced model

$$H_q(t,x) \equiv A{\cdot}K_q\left(\frac{t}{\tau}\right)_q Sin(\gamma{\cdot}x), \qquad F_q(t,x) \equiv \frac{\partial^2 H_q}{\partial t^2} = \frac{A\cdot q}{\tau^2}K_q\left(\frac{q^2 t}{\tau}\right)_q Sin(\gamma{\cdot}x) \tag{3.5}$$

where $F_q(t,x)$ is the initial forcing. After the initial forcing, we can see creation and propagation of tsunami waves going outward in both the positive and negative x directions from the point of the incident. This enables us to get a unique solution $\Phi(t,x)$ to the forced wave equation. [9] shows us that we can define two phase functions that correspond to the left and right propagation, where the parameters are related by $v_0\gamma\tau = q^\mu$.

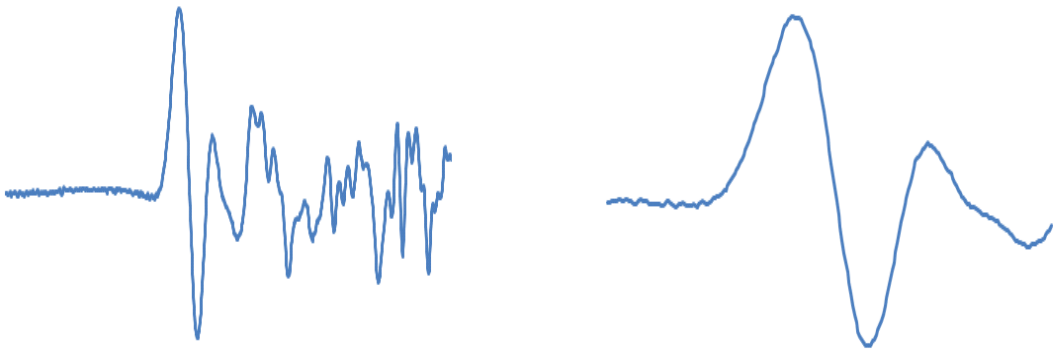

Figure 3: The 2011 Japaneese tsunami wave measured by DART 46411 (Left) Starting March 11, 1:30pm local time, to March 11, 5:40pm local time; (Right) Tsunami wavefront over one hour period.

Figure 3 shows a wavelet approximation of a tsunami. Note that it is not symmetric. The model of a rogue wave, shown later, is symmetric by necessity. We will compare this approximation to the actual data obtained from the tsunami that hit Japan in 2011 in a later chapter.

3.2 A symmetric two-sided rogue-like wavelet

What is needed for rogue waves are functions that have a large peak in the middle, but damp down quickly. The reason for this is the structure of a rogue wave. Remember, a tsunami is a fast-moving, low-amplitude wave. A rogue wave is opposite that; it is a slower moving, high amplitude wave whose forcing is brought about by resonance instead of a sharp and immediate forcing. As a result (and we will see this in later images), the wavelet profile of a rogue wave closely resembles a damped cosine function and is very symmetrical, whereas a tsunami's profile will be asymmetric. As there have been so very few of these measured, debate still rages about their cause. If we use a MADE-generated solution to construct a localized plane wave for $A > 0$, we arrive at

$$\Psi_q(t,x) = A \cdot {}_qCos\left(\frac{t}{\tau}\right) \cdot {}_qCos(\gamma \cdot x) \tag{3.6}$$

Substitution of this into the forced wave equation yields a small but persistent forcing. In this case, γ and τ are parameters that satisfy $v\gamma\tau = 1$ for a constant speed $v > 0$.

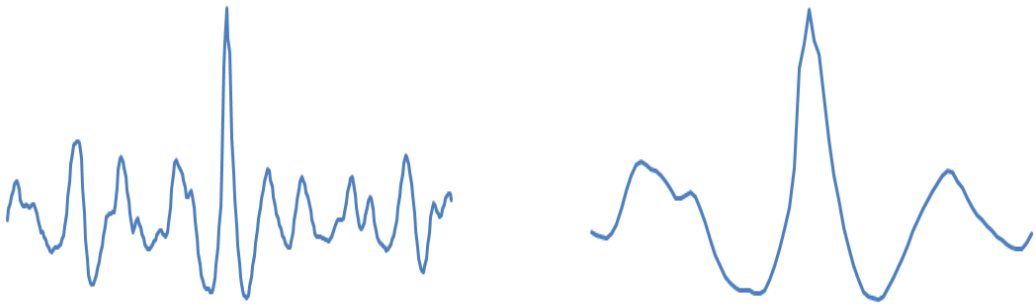

Figure 4: The 1995 Draupner rogue wave, or New Year's freak wave
(Left) 15 minute recording of the rogue wave;
(Right) Rogue wave closeup.

Figure 4 is a wavelet approximation of a rogue wave. This will be compared to

data from the Draupner rogue wave, one of very few that have been measured, from New Year's Day 1995 [9]. We will also be able to see the model of a resonance triad, the force we theorize is responsible for creating such waves, in the next chapter.

CHAPTER 4: Numerical modeling

In this section we will give the details of which equations were used to obtain numerical solutions

4.1 The Forced Wave Equation

Now, up to this point we have heard about forcing, but have given no actual information on exactly what we are talking about. In the tsunami case, it can be an earthquake or landslide, while in the case of a rogue wave it is a resonance triad. But how do we explain it mathematically? We can answer this question with the **forced wave equation**. Consider the forced one-dimensional wave equation for the water-level function Ψ:

$$\partial_t^2 \Psi(t,x) - v_0^2 \partial_x^2 \Psi(x,t) = F(t,x), \qquad \text{and} \qquad \Psi(x,t) = 0 \ \forall t < 0, \ x \in \mathbb{R} \tag{4.1}$$

We can see that the equation on the right will account for the boundary and initial conditions. Thus we have a one-dimensional wave equation that can account for the forcing of our waves.

4.2 The one-dimension Tsunami Models

A tsunami is physically the consequence of a spontaneous event on the seabed. The inciting event causes the creation of a variable pressure field throughout the volume of the water; this sets up forces at the surface of the ocean that causes local oscillations [9]. We are not as concerned with the behavior of the tsunami towards the shore as we are with its creation. Now, a tsunami wave can start as a result of earthquakes or landslides at or near the ocean floor. These displace the surface of the water due

to a forcing field $F(t, x, y)$ caused by a variability of $H(t, x, y)$. Here we will choose a model that considers a short-lived earthquake along a fault line defined by $x = 0$. The height and forcing depend on a parameter $q > 1$. For the forcing that creates the tsunami, we use the following equation:

$$\frac{\partial^2 \eta}{\partial t^2} \; - \; v_0^2 \frac{\partial^2 \eta}{\partial x^2} \; = \; F(t, x) \tag{4.2}$$

This equation allows us to get a graphical representation of the forcing that creates a tsunami.

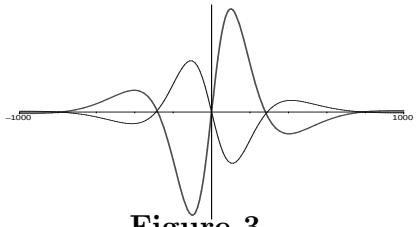

Figure 3

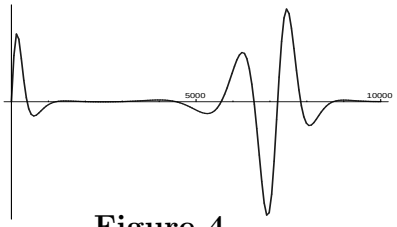

Figure 4

In Figure 3, an initial forcing has registered. We can see from Figure 4 that this has resulted in two waves being propagated from the center. From here, we will follow one wave, as the motion of the other will be similar. There was a tsunami wave that propogated out in the other direction, but we need only follow the motion of one. So as the wave propagates, it maintains a constant speed as long as the seafloor remains relatively constant. We use the following equation to model the propagation of a tsunami wave after t seconds:

$$\frac{\partial \eta}{\partial t} \; + \; v_0 \frac{\partial}{\partial x} \left(\eta + \frac{\beta}{v_0} \eta^2 + \frac{\gamma}{v_0} \frac{\partial^2 \eta}{\partial x^2} \right) \; = \; 0 \tag{4.3}$$

This is an equation that models the behavior of a soliton as it propagates away from its forcing! This equation is used for one-dimensional motion, so we don't have to go into the 2D one we mentioned earlier. That one would come in to play during

the runup of the NC coast we have a model of in the next section. So, now we can see forcing and propagation.

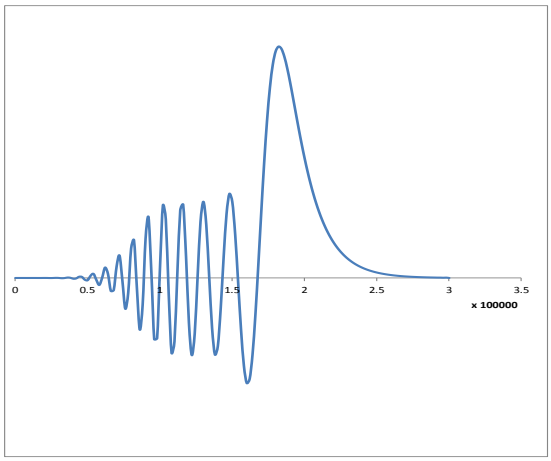

Figure 5

In Figure 5 we have modeled the propagation of the tsunami wave at $t = 5000s$. As it comes into shallower waters, the bottom, unseen part of the wave contacts the immovable seafloor, resulting in the bottom of the wave encountering a stark drop in speed. So now all of the lower portion of the wave is bunching up due to the encounter with the immovable seafloor, but the top of the wave does not lose celerity. Thus, the wave height increases and it crests over. The equation we use to model our runup is

$$\frac{\partial \eta}{\partial t} + v\frac{\partial \eta}{\partial x} + \frac{\eta}{2}\frac{dv}{dx} + \beta\frac{\partial(\eta^2)}{\partial x} + v_0\frac{\partial^3 \eta}{\partial x^3} \;=\; 0 \tag{4.4}$$

This gets more complicated when H depends on both x and y. That would be a situation where we would utilize the 2-Dimensional Water Wave Equation.

4.2.1 Wavelet analysis of the tsunami model

To detect, analyze, store, and recover a tsunami waveform, we will utilize a wavelet analysis. This is a very common approach [9] to this issue. We start by identifying a wavelet frame, a concept mentioned in the previous chapter:

$$\Lambda_\Psi \equiv \{q^{j/2}\Psi(q^j t - kb)/||\Psi|| \ : \ j,k \in \mathbb{Z}\}.$$

From [9] we see this leads to a wavelet transform $W_\Psi : \mathcal{L}^2(\mathbb{R}) \to l^2(\mathbb{Z}^2)$ where

$$W_\Psi[f](j,k) \ \equiv < \Psi_{j,k}, f > = \int_{\mathbb{R}} \Psi(q^j t - kb) f(t)\ dt\ .$$

And thus for our wavelet frame, we have:

$$\Lambda_{K_q} \ = \ \left\{ \sqrt{q^j/C_K} \cdot K_q(q^j t - kb) \mid j,k \in \mathbb{Z} \right\}, \qquad C_K \ \equiv \ \int_0^\infty K_q^2(t)\ dt\ . \tag{4.5}$$

What we end up with is a fram of asymmetric wavelet profiles. The Haar wavelet is also asymmetric. However, unlike the Haar basis, the frame in (4.5) is not orthonormal in $\mathcal{L}^2$. Still, we will see in later sections the results of applying this wavelet frame to NOAA data from an actual measured tsunami, and the outcome is quite reasonable.

4.3 The two-dimension Tsunami Models for the NC coast

Here we use a depth profile $H(x,y)$ that is similar to Cape Hatteras in North Carolina (see Figure 6).

The result indicates that water-wave heights would increase most at the capes, in the event that a tsunami hit the NC coast. The possibility resides with an unstable,

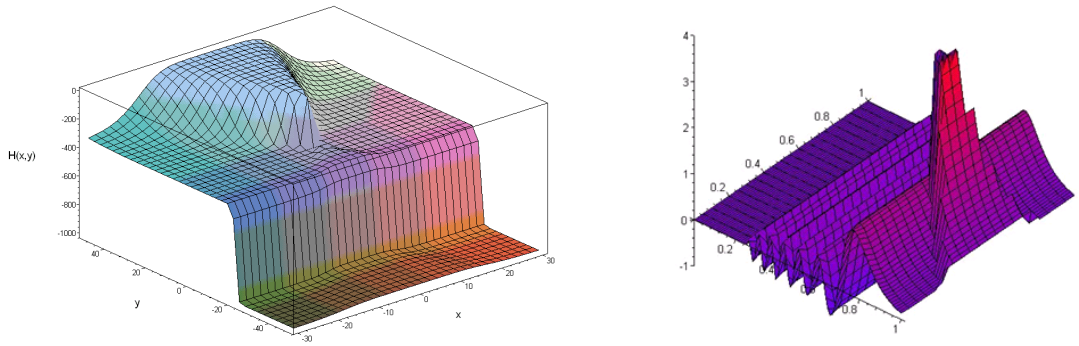

Figure 6: (Left) Seafloor profile model $H(x, y)$ for the NC coast near Cape Hatteras; (Right) Wave height as obtained from the 2-D numerical solution of the KdV equation using speed $v(x, y) = \sqrt{Hg}$.

but dormant volcano in the Canary Islands.

4.4 Rogue wave models and resonances

The concept of a resonance triad is discussed in [5]. A resonance triad is when two wave frequencies sum to a third. The resulting wave is larger than the two whose frequencies combined. This is the natural outcome of rippling surface waves that propogate in different directions creating a constructive interference. We believe this to be a mechanism that causes rogue waves, though their origin is still under debate. It can be shown, however, that small amplitude forces over a long period of time can naturally produce large rogue waves [9]. If we substitute (3.6) into (4.1), we get:

$$\partial_t^2[A \cdot {}_qCos(t/\tau) \cdot {}_qCos(\gamma \cdot x)] - v_0^2\partial_x^2[A \cdot {}_qCos(t/\tau) \cdot {}_qCos(\gamma \cdot x)]$$

$$= \frac{A}{\tau^2}\ {}_qCos(q \cdot \frac{t}{\tau}) \cdot {}_qCos(\gamma \cdot x) - Av_0^2\gamma^2\,{}_qCos(\frac{t}{\tau}) \cdot {}_qCos(q \cdot \gamma \cdot x)$$

And, as we have established that $v_0\gamma\tau = 1$, we get the forcing equation for a rogue wave being:

$$F_q(t,x) \;=\; A\gamma^2 v^2 \cdot [{}_qCos(q \cdot \frac{t}{\tau}) \cdot {}_qCos(\gamma \cdot x) - {}_qCos(\frac{t}{\tau}) \cdot {}_qCos(q \cdot \gamma \cdot x) \qquad (4.6)$$

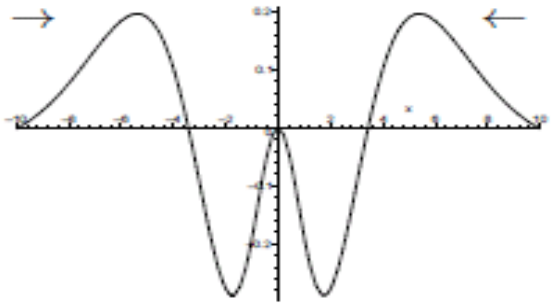

Figure 7

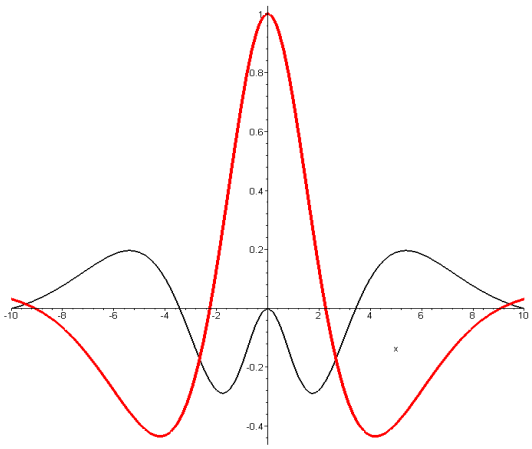

Figure 8

In figure 7, we see two counter-propagating waves of similar frequency. Recall that this is a factor in the resonance triad that we claim forces the creation of a rogue wave. After these waves combine, they form a much larger wave. In figure 8, the black graph models the counter propagating wave, while the red one is the resultant rogue wave.

4.4.1 Wavelet analysis of the rogue model

Using the forcing equation from earlier, (4.6), we are able to model the resonance triad that causes the rogue wave:

As we can see from the figures above, the two counter-propagating waves come together, and their frequencies produce a much larger wave.

Recall what we discussed earlier about a rogue wave. Unlike a tsunami, which is

a low-amplitude, high speed wave, a rogue wave is a high-amplitude, low speed wave. There might be a speed $s << v$ to the wave-height profile when a slight drift in the rogue-generating current is present. A model for such a wave can be given, from [9], by

$$\Psi_{q,s}(t,x) \equiv A \cdot {}_qCos(\Gamma_s \cdot \gamma \cdot vt) \cdot {}_qCos(\gamma \cdot (x - st)) \tag{4.7}$$

We'll get an idea for how these are modeled in the Signal Analysis chapter.

CHAPTER 5: Signal analysis of data

Here we use the wavelet analysis techniques to consider the specialized situation address in this thesis.

5.0.2 Tsunami data

We consider tsunami data obtained from NOAA in 2011. In order to model a tsunami, a one-sided, non-symmetric profile is used. The resultant data yields the following results. For the charts below, the discrete scale variable j is our vertical axis, while the discrete shift variable k is our horizontal axis:

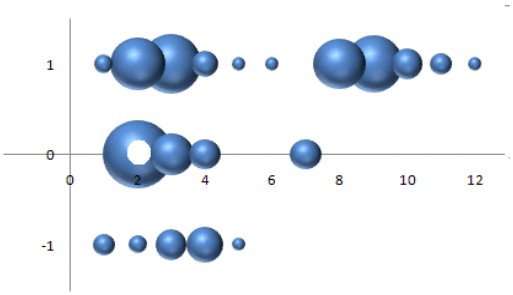

Figure 9

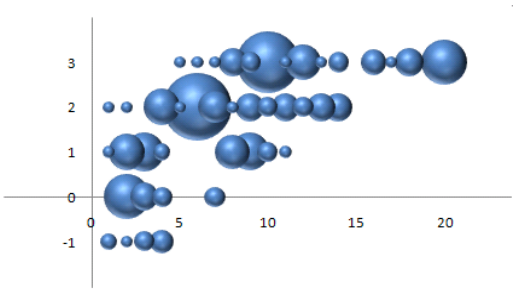

Figure 10

Figures 9 and 10, from [9], are wavelet analyses of the Japan tsunami of 2011. Note that the balls in these charts are of varying size. Recall that in the wavelet chapter, we covered using a wavelet transform to find discrete coefficients $C_{j,k}$ of Ψ. Well, the size of these coefficients is directly related to the size of the ball on the graph. Here we have two different bubble charts, but only one tsunami. The only difference in the two is the amount of coefficients chosen to graph. For Figure 9 we see the 20 largest magnitude coefficients in a range of $-1 \leq j \leq 1$ and $1 \leq k \leq 12$, while the second chart is approximately 40 of the largest magnitude coefficients for $-1 \leq j \leq 3$ and $1 \leq k \leq 20$. In their article containing the analysis of this tsunami,

Pravica, Randriampiry, and Spurr choose the wavelet frame,

$$\Lambda_{K_q} = \{\sqrt{q^j/C_K} \cdot K_q(q^j t - kb)|j,k \in \mathbb{Z}\} \text{ for } C_K \equiv \int_0^\infty K_q^2(t)\, dt,$$

where $q = 1.5$ and $b = 1.95$. With this data, we can reconstruct the tsunami's wavelet profile and compare it to the actual data:

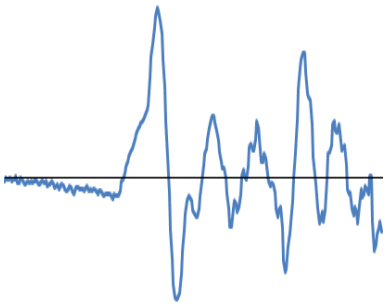

Figure 11

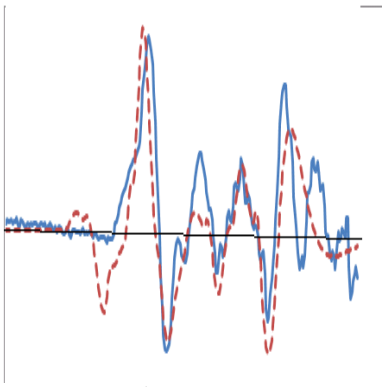

Figure 12

These two figures were obtained from [9]. The figure on the left is from the actual wave profile of the actual tsunami. On the right, we have the two results graphed together for comparison. The blue solid line is the actual data, while the red dotted line is the result arrived at by [9]. For their result, they took only the 20 largest ocefficients in magnitude; the normalized RMS error was 16% [9] They are, as can be seen, very similar.

5.0.3 Rogue data

We consider rogue data obtained from the Draupner platform in 1995. We use the symmetric q-Cosine function for the rogue wave profile.

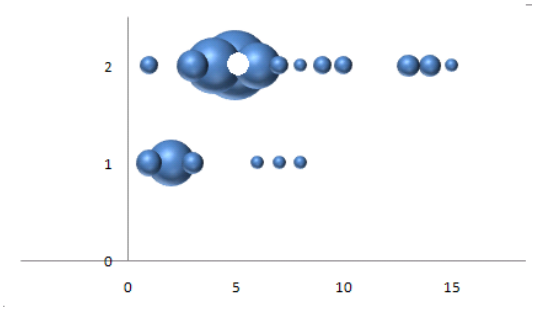

Figure 13

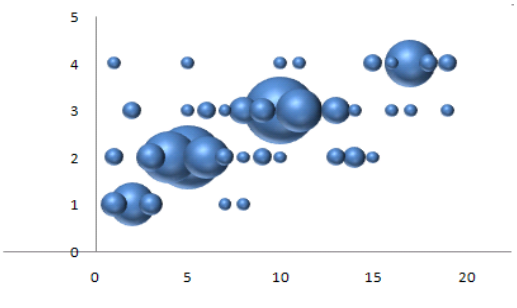

Figure 14

These two figures were also obtained from [9]. Like the bubble graphs of the tsunami data, these show the largest magnitude coefficients from the discretized data. The wavelet frame for the rogue wave utilizes the ${}_qCos$ function shown previously. The frame used in [9] is,

$$\Lambda_{{}_qCos} \;=\; \{\sqrt{q^j/C_C}\cdot {}_qCos(q^j t - kb)|j,k \;\in\; \mathbb{Z}\}\;,\; \text{for } C_C \;\equiv\; \int_0^\infty {}_qCos^2(t)\;dt,$$

where this time $q = 1.5$ and $b = 2.44$. Like the tsunami profile, these two charts show the same data with different amounts of coefficients from the discretized data; Figure 13 shows approximately 20 coefficients in the range of $0 < j \leq 2$ and $0 < k \leq 12$, while Figure 14 shows approximately 40 coefficients within $0 < j \leq 5$ and $0 < k \leq 20$. Using the wavelet analysis modeled by the above figures, we can reconstruct the wave.

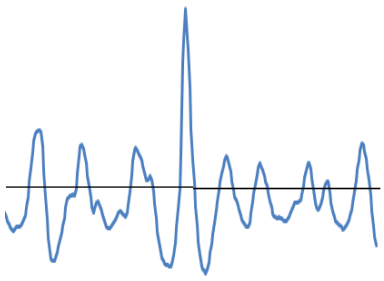

Figure 15

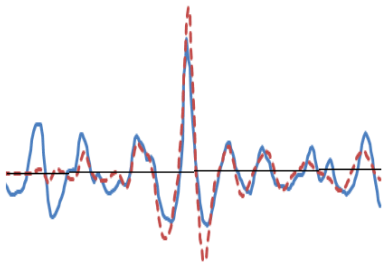

Figure 16

These figures were obtained from [9]. The Draupner data is shown in Figure 15, while the figure on the right is graphed with the wavelet analysis as the red dotted line. 30 coefficients were used for the wavelet data, with a normalized RMS error of 18% [9].

CHAPTER 6: Comprisons and Conclusions

The wavelet analyses of Tsunami and Rogue waves show the connection between numerical solutions and actual data. As shown in the figures, the wavelet analysis matches very close with already established methods of measuring these phenomena. The wavelet analysis is a very efficient way of modeling these data; it shows that using only the largest coefficients from discretized data, one can still model a tsunami or rogue wave within an acceptable error rate and arrive at a similar profile as the available data. Additionally, if one wants less error, one need only add more coefficients to the profile and it will match that much more closely.

REFERENCES

[1] Arfken (2010). *Mathematical Physics*. Cambridge University Press, Cambridge, fifth edition.

[2] Carrier, G. F. and Pearson, C. E. (1988). *Partial Differential Equations Theory and Technique*. Academic Press, Inc., San Diego, California, second edition.

[3] Gill (1982). *Atmosphere-Ocean Dynamics*. Academic Press, Boston, MA.

[4] Hai-Qiang, Z., Xiang-Hua, M., and Juan Li, B. T. (2008). Soliton resonance of the (2+1)-dimensional boussinesq equation for gravity water waves. *Nonlinear Analysis: Real World Applications*, 9:920–926.

[5] Halliday, D., Resnick, R., and Walker, J. (2005). *Fundamentals of Physics*. John Wiley and Sons, Inc., Hoboken, New Jersey, seventh edition.

[6] Holton (2006). *An introduction to dynamic meteorology*. Elsevier Academic Press, Boston, MA, 4 edition.

[7] Johnson, R. (1980). Water waves and the korteweg-de vries equations. *J. Fluid Mech.*, 97(4):701–719.

[8] Pravica, D., Randriamiry, N., and Spurr, M. (2008). Applications of an advanced differential equation in the study of wavelets. *Applied and Computational Harmonic Analysis*, 27(1):2–11.

[9] Pravica, D., Randriamiry, N., and Spurr, M. (2011). A family of models for tsunami and rogue waves from solutions of q-advanced differential equations. (1).

[10] Pravica, D., Randriamiry, N., and Spurr, M. (2012). Reproducing kernel bounds for an advanced wavelet frame via the theta function. *Applied and Computational Harmonic Analysis*.

[11] Press, W. H., Teukolsky, S. A., Vetterling, W. T., and Flannery, B. P. (2007). *Numerical Recipes, The Art of Scientific Computing*. Cambridge University Press, Cambridge, third edition.

[12] Weir, M. D., Hass, J., and Giordano, F. R. (2005). *Thomas' Calculus*. Pearson Education System, Boston, MA, eleventh edition.